Available online at www.sciencedirect.com
ScienceDirect
Optical Materials 29 (2007) 1075–1083
OPTICAL Materials
www.elsevier.com/locate/optmat

Effect of IR femtosecond laser irradiation on the structure of new sulfo-selenide glasses

L. Petit [a,*,1], N. Carlie [a,1], T. Anderson [a], M. Couzi [b], J. Choi [a], M. Richardson [a], K.C. Richardson [a,1]

[a] College of Optics and Photonics CREOL/FPCE, University of Central Florida, Orlando, 4000 Central Florida Boulevard, FL 32816, USA
[b] Laboratoire de Physico-Chimie Moleculaire (LPCM), UMR 5803, CNRS 351, cours de la Liberation, 33405 Talence Cedex, France

Received 6 February 2006; accepted 17 April 2006
Available online 10 July 2006

Abstract

We report results of a systematic study to evaluate for the first time, the relationship between compositional variation and photo-sensitivity of new glasses in the Ge–Sb–S/Se system with varying ratios of chalcogen (S/Se), upon IR femstosecond laser exposure. It is shown that the photo-sensitivity of the glass depends on the glass composition and that IR femtosecond laser irradiation in this system results in near-surface photo-expansion. Glass structure modification as a function of S/Se ratio and the influence of laser dose has been characterized using micro-Raman spectroscopy and is correlated to the resulting photo-expansion. As compared to other widely studied binary chalcogenide glass systems, photo-expansion was found to vary with the Se content. Such modification opens the pathway towards the laser writing of photonic devices in the surface of the material.

Keywords: Germanium-based sulfide glass; Raman spectroscopy; Femtosecond laser irradiation; Photo-expansion; Photo-sensitivity

1. Introduction

Direct laser writing of photonic structures in transparent optical media has drawn considerable attention since the development of femtosecond lasers and the recognition of their ability to modify the properties of optical materials [1]. One of the principal applications of this technology is towards the fabrication of optical waveguides. The use of focused femtosecond laser pulses to produce structural modification in optical glasses is now well known [1–5]. In this regime the focused intensity within the material must reach a certain value, depending on the material, for a structural change to occur. Initially these intensities could be achieved with only ~100-fs Ti:sapphire lasers employing chirped-pulse amplification in conjunction with a regenerative or multipass amplifier, producing pulses at kilohertz repetition rates with micro-Joule energies. Depending on the desired photo-induced structural change, there are advantages of using femtosecond regime over the nanosecond regime. These advantages lie in its ability to deposit energy into a material in a very short time period, before thermal diffusion can occur. As a result, the heat-affected zone (HAZ), where melting and solidification can occur, is significantly reduced, leading to structured features that (i) are smaller in size, (ii) have higher aspect ratios, and (iii) have greater spatial precision. Exposed at intensities below ablation threshold, many materials exhibit non-linear absorption. This induces some structural changes, either in the surface or in bulk material leading to the ability to create three-dimensional structures, active devices in waveguides or complete optical systems on a single chip. It is now recognized that these processes and effects can be utilized to make a number of interesting and potentially useful micro-devices.

* Corresponding author. Tel.: +1 864 656 1259; fax: +1 864 656 1099.
E-mail address: lpetit@clemson.edu (L. Petit).
[1] Present address: School of Material Science and Engineering, Clemson University, Clemson, SC 29634, USA.

0925-3467/$ - see front matter © 2006 Elsevier B.V. All rights reserved.
doi:10.1016/j.optmat.2006.04.008

Most studies that use femtosecond direct laser writing have investigated waveguide fabrication in oxide glasses, based primarily silicate and phosphate matrices [2,3,6,7] and a few in polymers [8]. In these applications, the modification requires high single pulse energies to realize bond distortion and/or defect formation. These energies are reduced in materials where bond strengths are lower, as in non-oxide media, such as chalcogenide glasses (ChGs). Clearly of interest is the mechanism whereby materials can be modified, as the direct result varies greatly with material type, exposure conditions and the linear and non-linear optical properties of the material.

Chalcogenide glasses exhibit several interesting properties that can be exploited for the fabrication of photonic devices. In particular, their excellent infrared transparency, their large non-linear refractive indices which are can be varied widely, with compositional changes [9], and their low phonon energies make ChGs good candidates over oxide glasses and single crystals for mid- and long-wave infrared (LWIR) applications. Despite their often limited thermal and mechanical stability, attributable to weaker bond strengths and thus lower glass transition temperatures, ChG materials have been widely studied for use in the fabrication of all-optical switches and as integrated optical elements. ChGs are also potential candidates for applications in reversible optical recording, as integrated optical elements [10], memory switching [11], inorganic photo-resists and antireflection coatings [12–14]. The most promising applications of these glasses are for transmission in the mid-IR (MIR) range (3–7 μm) for optical communication systems [15]. Previous studies have shown that optical waveguides in As–S–Se-based ChGs can be fabricated by several techniques, including photo-lithography, ion implantation, and laser beam writing [16].

Germanium-based chalcogenide glasses containing heavy metal species such as antimony have also been well studied for their potential as glasses with high non-linear optical properties [17,18]. Selenide materials have also been identified as possible materials for non-linear optical applications [19,20]. Several investigations have mentioned that the introduction of selenium to the As–S system increases the non-resonant non-linear refractive index (n_2) up to 400 times the n_2 for fused silica [21]. An increase of n_2 with an excess of S/Se content has been also observed in As–S–Se glass system and has been correlated with the presence of covalent, homopolar Se–Se bonds in the glass structure.

This study aims to broaden the understanding of the linear and non-linear optical material properties and the influence of such on the material's photo-sensitivity, or photo-response, in other families of ChG materials. With these results, a progressive understanding of the driving mechanisms and material potential can be realized, thereby broadening their use in more diverse applications. We have examined glasses in the Ge–Sb–S system with a low Sb concentration and with an excess of S, which possess good physical stability and high non-linear index suitable for use in novel optical applications. In order to increase the non-linear refractive index, Sulfur has been replaced progressively by Selenium. Glasses in the host system $Ge_{0.23}Sb_{0.07}S_{0.70-x}Se_x$ with $x = 0$, 0.05, 0.10, 0.20, 0.50 and 0.70 have been investigated. The correlation between the glass structure and the optical properties of the glasses has already been reported [22]. Nevertheless, no systematic study has been conducted to our knowledge on the response of these materials under IR femtosecond laser irradiation and the composition dependence on such photo-sensitivity.

In this paper, the photo-sensitivity of these new glasses with varying S/Se ratios is compared following femtosecond laser exposure 800 nm. In particular, we describe the use of MHz femtosecond (62 fs) laser pulses trains of only nanoJoules of energy for creating micron-size square surface relief features in these glasses. Such surface features can then be readily characterized to gain insight into resulting laser-induced modification of structural changes. Micro-Raman spectroscopy has been employed to verify the structural modification of the glasses after laser irradiation. Understanding the relationship between the optical properties and the response of the ChG under laser irradiation is a prerequisite toward the successful development of laser waveguide writing in these glasses. We examine the material response in the bulk glasses, and also discuss the potential uses for thin films of these materials for planar waveguides.

2. Experimental

2.1. Glass elaboration and analysis

Sulfide glasses in the glass host system $Ge_{0.23}Sb_{0.07}S_{0.70-x}Se_x$ with $x = 0$, 0.05, 0.10, 0.20, 0.50 and 0.70 were examined in this study and were prepared in 15 g batches. The sulfide glasses were prepared from high purity elements (Ge Aldrich 99.999%, Sb Alpha 99.9%, S Cerac 99.999% and Se Cerac 99.999%). The starting materials were weighed and batched inside a nitrogen-purged glove box and sealed using a gas—oxygen torch under vacuum into quartz ampoules. Prior to sealing and melting, the ampoule and batch was pre-heated at 100 °C for 4 h to remove surface moisture from the quartz ampoule and the batch raw materials. The ampoule was then sealed and heated for 24 h to between 800 and 950 °C, depending on the glass composition. A rocking furnace was used to rock the ampoule during the melting to increase the homogeneity of the melt. Once homogenized, the melt-containing ampoule was air-quenched to room temperature. To avoid fracture of the tube and glass ingot, the ampoules were subsequently returned to the furnace for annealing for 15 h at 40 °C below the glass transition temperature, T_g. The same procedure was used for selenium-substituted compositions.

The use of elemental dispersive spectroscopy (EDS) verified that the elemental compositions of the glasses were identical to the initial concentrations of species introduced

in the batch. No loss of sulfide was observed within the accuracy of the measurement (±2%).

2.2. Spectral characterization of the investigated glasses

The absorption spectrum of each sample was recorded at room temperature. Vis–IR absorption spectra were measured using a spectrophotometer using 2 mm thick optically polished samples.

Micro-Raman scattering spectroscopy was used to determine the structural modification in the glasses after IR femtosecond laser irradiation. Raman spectra were recorded with a LabRam confocal micro-Raman instrument from JOBIN-YVON (typical resolution of 2–3 cm^{-1}), in back-scattering geometry at room temperature. The system consists of a holographic notch filter for Rayleigh light rejection, a microscope equipped with 10×, 50× and 100× objectives (the latter allowing a spatial resolution of less than 2 μm), and a CCD detector. The 752 nm emission line of an argon-krypton laser was used for excitation with incident power of around 10 mW. The use of a 752 nm source was specific to our study in that the excitation wavelength was made at an energy well below the bandgap region for most of our samples.

2.3. Femtosecond laser irradiation setup

The laser oscillator used for the writing process in this study is an extended-cavity Ti:Sapphire laser with a repetition rate reduced to 35.8 MHz and an ~25 nm spectral bandwidth centered at 810 nm that produces 8 nJ pulses with 62 fs duration and 6% pulse-to-pulse stability. The Gaussian laser output beam (M^2 of ~2.6) was focused by a 10×, 0.25-N.A. microscope objective at the surface of the bulk sample that was translated perpendicular to the laser beam by a computer-controlled three-axis translation stage. Squares were written at the surface of the samples by translation of the bulk material transversally with respect to the focused laser beam by use of a three-dimensional motorized translation stage. The exposed regions consisted of 100 μm-by-100 μm squares made by scanning 50 lines spaced 2 μm apart at a rate 10, 20, 50 and 100 μm/s upon the laser focal spot area, allowing the number of pulses incident upon the laser focal spot area to be varied (among different squares) for different laser intensities. The laser intensity was adjusted with a variable metallic neutral-density filter placed before the microscope objective. The resulting photo-modified surface profile was then analyzed with a white-light interference microscope (Zygo instrument NewView5000) to assess photo-induced surface modification.

3. Results and discussion

The purpose of this study was (i) to show for the first time, to our knowledge, that sulfo-selenide bulk glasses within this glass system are photo-sensitive under IR femtosecond laser irradiation, (ii) to characterize and understand the glass network modification created by laser irradiation, and (iii) to evaluate the compositional variation of such response with changing chalcogen content to more thoroughly assess the modification's mechanism. With such an understanding, the fabrication of photo-induced waveguides in these matrices might then be possible.

In order to obtain photo-induced waveguides of good quality in these bulk materials, we first determined the threshold between ablation and photo-induced spot writing by independently increasing the laser intensity and exposure time until ablation was observed. Once this composition-dependent threshold was determined within the glass compositional series examined, we fabricated irradiated squares made of multiple photo-induced scanned lines. Squares were written at various intensities below the ablation threshold, large enough to be able to measure the micro-Raman spectra of the irradiated region and to assess structural modification via spectroscopic techniques.

3.1. Determination of the ablation threshold

The goal of the ablation threshold determination experiment is to observe the variation in photo-modified glass properties with respect to the original bulk material properties, to understand the compositional effect on the resulting material photo-sensitivity for bulk glasses and finally, to assess the exposure condition's (intensity or dose) influence on the properties for each composition. The threshold for the onset of ablation as compared to non-ablative photo-modification was determined by irradiated separate spots with a specific number of pulses, followed by incrementally increasing the laser intensity resulting in a two-dimensional map. Fig. 1(a) shows a photo-micrograph map of these spots for the glass $Ge_{0.23}Sb_{0.07}S_{0.70}$ surface, utilizing a 50× microscope objective. Apparent is the systematic variation in material response, as noted by the exposed region's appearance, as a function of dose. The ablation threshold is not only function of the laser intensity but also of the dose or accumulated number of laser shots for a given exposure time. It can be seen, however, that the sample surface seems to be more sensitive to the laser intensity than to the dose. Fig. 1(b) presents the surface profile of the holes corresponding to the black spots showing that the glass was ablated. When the laser intensity is decreased below the ablation threshold, photo-expansion spots are observed. The threshold between ablation and photo-induced writing has been estimated for the glass $Ge_{0.23}Sb_{0.07}S_{0.70}$ to be ~169 GW/cm^2. Similar determination of the ablation thresholds for the other glasses investigated is shown in Fig. 2 as a function of the Se content. As previously observed with glasses in the As–S–Se system [23,24], the ablation threshold decreases dramatically with the progressive replacement of S by Se. This result must be related to the red shift of the absorption band gap with the progressive introduction of Se, as presented in Fig. 3.

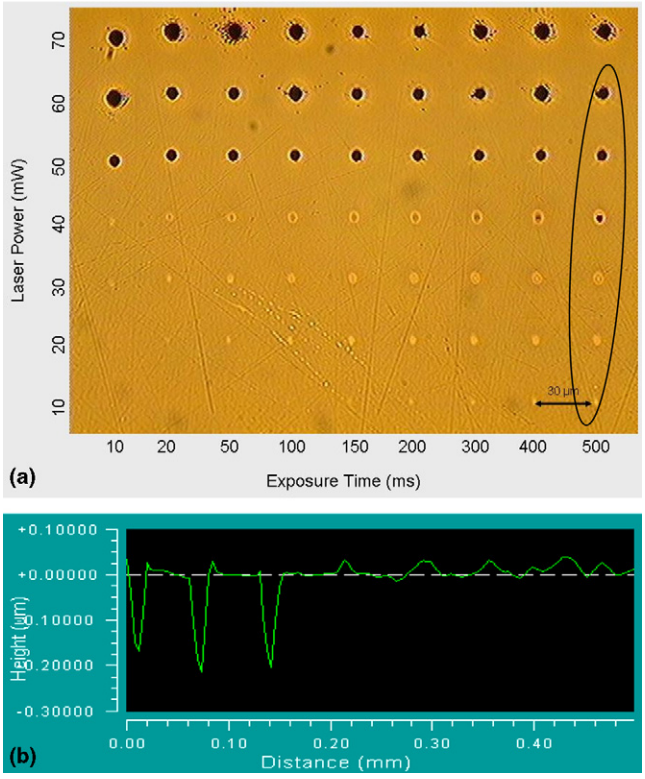

Fig. 1. Image (a) and surface profile (b) of the glass $Ge_{0.23}Sb_{0.07}S_{0.70}$ using Zygo New View white light interferometer microscope.

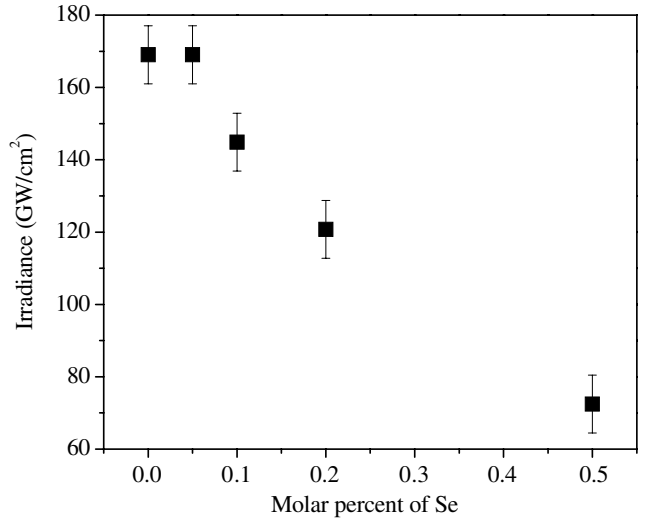

Fig. 2. Ablation threshold of the glasses in function of the selenium content.

Indeed, the laser irradiation induces multiple photon absorption for the pure sulfide glass and only single photon absorption for the pure selenide glass.

3.2. Photo-expansion versus S/Se ratio

Fig. 4 shows an irradiated square 100 µm × 100 µm in size, made from multiple adjacent photo-induced line scans

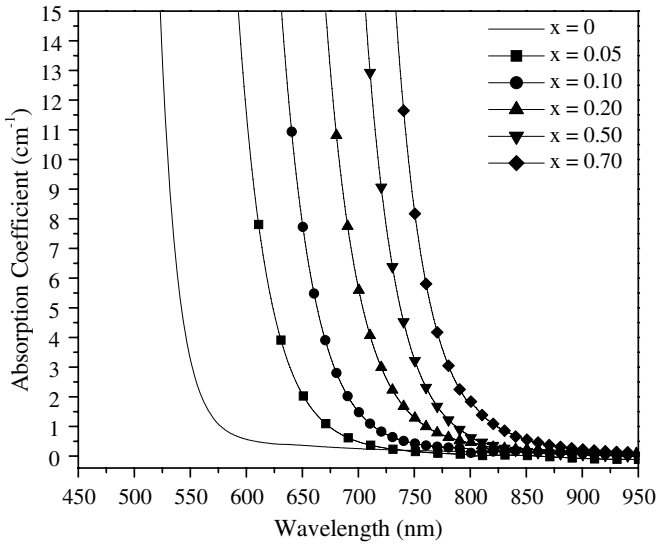

Fig. 3. Absorption spectra of glasses in the system $Ge_{0.23}Sb_{0.07}S_{0.77-x}Se_x$.

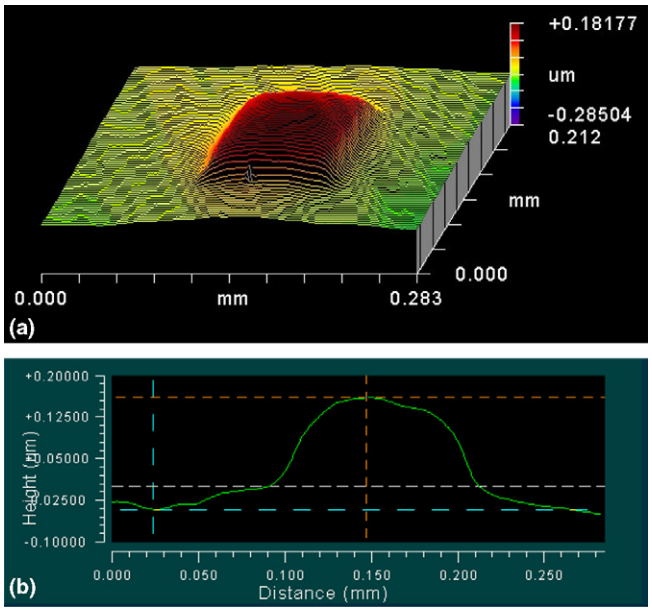

Fig. 4. Image of a square written at the surface of $Ge_{0.23}Sb_{0.07}S_{0.60}Se_{0.10}$ (a) and its surface profile (b) using Zygo New View white light interferometer microscope.

along the surface of a bulk $Ge_{0.23}Sb_{0.07}S_{0.60}Se_{0.10}$ glass sample. This specimen was processed at the ablation threshold with a translation speed 20 µm/s. The dose, corresponding to the irradiance of the laser at the ablation threshold divided by the translation speed, is ~88.9 MJ/cm^3. Fig. 5 shows the photo-expansion of the irradiated squares written at the ablation threshold irradiance of each glass using different translation speeds. One can observe an increase of the photo-expansion with a decrease of the translation speed corresponding to an increase of the total exposure *dose*. The pure sulfide glass exhibits higher photo-expansion than the Se contained glass. A progressive decrease of the photo-expansion has

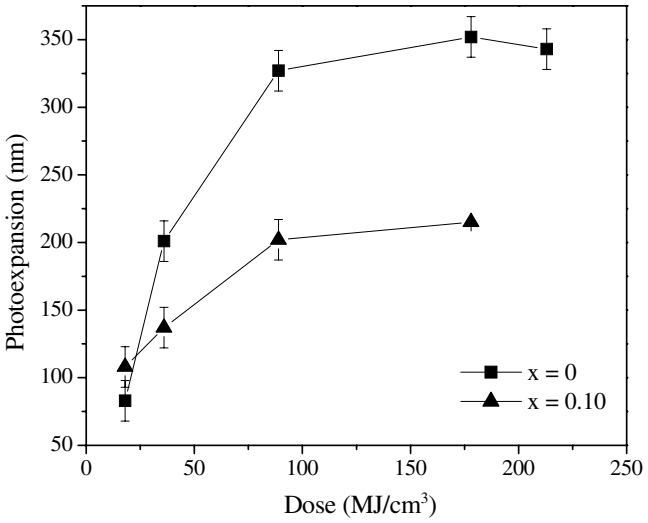

Fig. 5. Photo-expansion of the investigated glasses as a function of laser exposure dose.

been observed during the 6 months following the irradiation exposure, indicating that the irradiation led only to reversible glass structure modification.

3.3. Effect of the laser irradiation on the glass structure

Before discussing the variation of the observed photo-expansion in the glasses examined, a brief description of the structural characteristics of the glasses as a function of Se content is presented. A detailed study of the Raman spectra of the glasses as a function of Se content has previously been reported [22].

Fig. 6 presents the micro-Raman spectra of the glasses with $x = 0$ and 0.10. All Raman spectra show a broad band in the range 300–500 cm^{-1}. Depending on the composition, the Raman spectra exhibit bands at around 210, 260, 330 and 475 cm^{-1}. When Se is incorporated in the glass network, the band located 330 cm^{-1} becomes broad and the intensity of the bands in the range 200–270 cm^{-1} increases. The band at around 200 cm^{-1} has been attributed to $GeSe_{4/2}$ tetrahedra as presented in Fig. 7(a) and the shoulder at 216 cm^{-1} to vibration of edge-sharing $Ge_2S_{8/2}$ bi-tetrahedra as illustrated in Fig. 7(b) [25]. Because of the presence of excess S, this band may be also related to the presence of mixed units like $GeSe_3S$ [26,27]. The shoulder at around 190 cm^{-1} has been attributed to heteropolar Sb–Se bond vibrations in the $SbSe_3$ pyramids [28]. The band 266 cm^{-1} corresponds to Se–Se bonds in chains. The shoulder observed at around 250 cm^{-1} may be related to Se–Se bonds in ring. In accordance with previous study in similar glass system [29], the broad band near 330 cm^{-1} is formed by different, individual Raman signals, which have been overlapped. The shoulder at around 302 cm^{-1} has been assigned to the E modes of SbS_3 pyramids. In accordance with Mei et al., the bands at 330 and 402 cm^{-1} have been assigned to the A_1 and T_2 modes of corner sharing $GeS_{4/2}$ groups (Fig. 7(a)) [30]. The bands at 340, 375 and 427 cm^{-1} have been attributed, respectively, to A_1 mode of the GeS_4 molecular units [31], to the T_2 mode of 2 edge-sharing $GeS_{4/2}$ tetrahedra and to the vibration of two tetrahedra connected through a bridging sulfur $S_3Ge–S–GeS_3$ [30]. The weak band near 450–500 cm^{-1} has been assigned to vibration mode of sulfur. The shoulder at around 475 cm^{-1}, more pronounced in the Raman spectra of the Se-containing glasses, may be attributed to the $S_8(A_1)$ ring vibration mode of sulfur. The band at 485 cm^{-1} has been related to vibration of $S(A_1)$ chain.

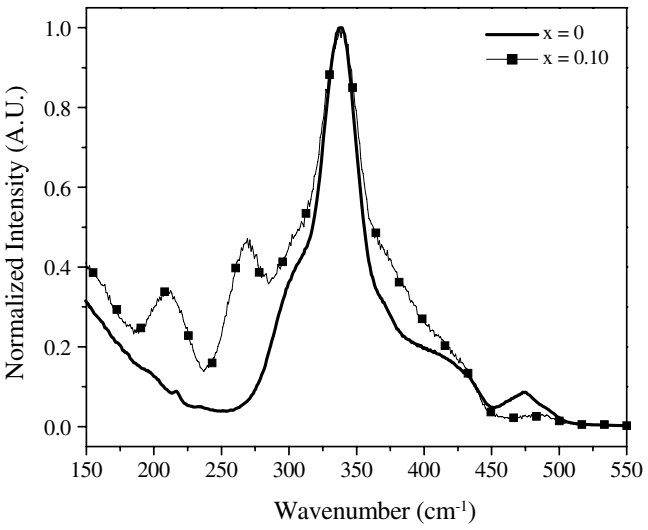

Fig. 6. Micro-Raman spectra of the glasses in function of x (Se).

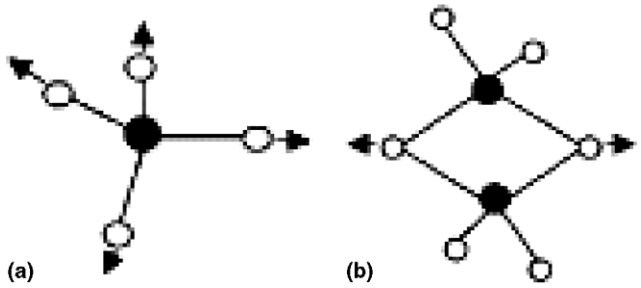

Fig. 7. Possible bonding configurations of GeX_4 units (x = S and/or Se) within glass matrix, with (a) corner-sharing and (b) edge-sharing arrangements.

When Se is introduced in the sulfide glass network, the main band becomes broader showing the connection of the GeS_4 tetrahedra. The amplitude of the bands at 375 and 425 cm^{-1} increases strongly showing connection of the GeS_4 units forming edge-sharing $GeS_{4/2}$ and $GeS_2S_{2/2}$ units. The intensity of the band at around 260 cm^{-1} increases dramatically showing the formation of Se in chains and rings.

3.3.1. $Ge_{0.23}Sb_{0.07}S_{0.70}$ glass

Fig. 8 presents the micro-Raman spectra of the glass with $x = 0$ and of the irradiated squares which were written

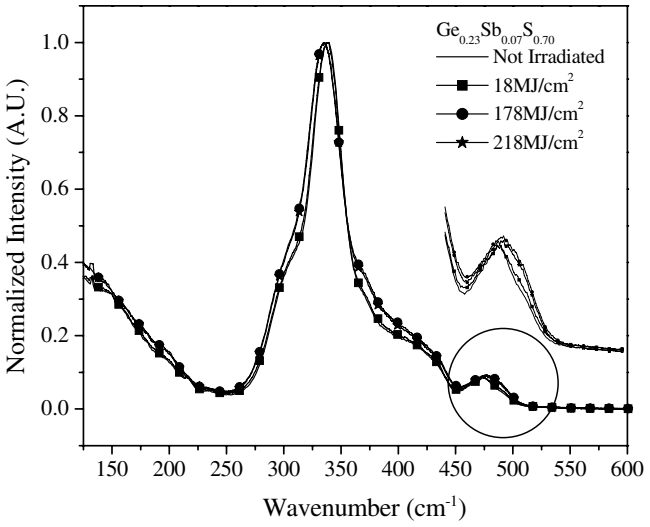

Fig. 8. Micro-Raman spectra of the non-irradiated and irradiated glass with $x = 0$.

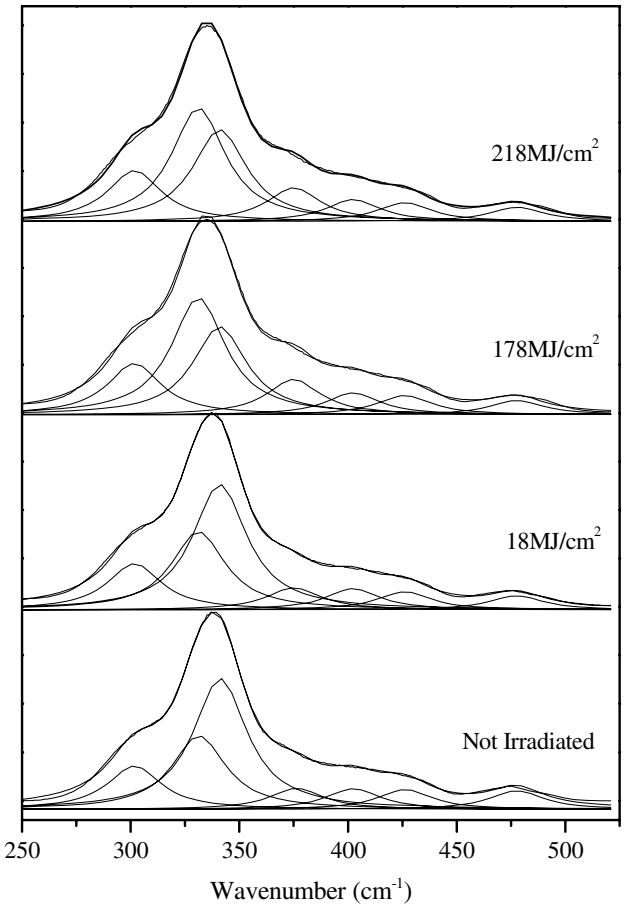

Fig. 9. Deconvolution of the micro-Raman spectra of the glass with $x = 0$ after different irradiations.

using different doses. When the dose increases, the broad band at 340 cm^{-1} shifts to lower wavenumber and becomes broader. One can notice that no band appears at 260 cm^{-1} showing the absence of Ge–Ge homopolar band creation after laser irradiation. The band located at 485 cm^{-1} exhibits a modest increase in intensity but as can be seen, this increase is significant compared to the changes observed in the band at 475 cm^{-1}, which becomes broader reflecting a small increase in S chains.

In order to understand the structural modification after irradiation, the main band was deconvolved, and results were found to be in agreement with Frumarova et al. [29]. The spectra and their fittings are presented in Fig. 9 and the relative fractions of each fit are given in Table 1. One can notice that the intensity of the bands located at 330 and 375 cm^{-1} increases with the increase of the dose whereas the intensity of the band at 340 cm^{-1} decreases. This indicates an increase of the connectivity between GeS_4 tetrahedra units which possess mainly cornered–shared units suggesting their S creates S–S chains. This is consistent with, and in accordance with the notable increase in intensity of the band at 485 cm^{-1}. The laser irradiation can be seen to modify the bonding configurations in the pure germanium sulfide glass by connecting the GeS_4 units through S–S chains as shown in Fig. 7(a):

$$GeS_4 + GeS_4 \rightarrow \text{–Ge–S–S–Ge–}$$

(this latter unit called $GeS_{4/2}$). The small increase of the bands at 375 and 475 cm^{-1} suggests the small, but measurable evidence that few GeS_4 units in the fs-modified glass connect by edge-sharing their S (as depicted in Fig. 7(b)) thus creating S–S connecting units such as those resulting from

$$GeS_4 + GeS_4 \rightarrow Ge_2S_{6/2} + S_2$$

To summarize, laser irradiation of the sulfur-containing glasses results in an increase of number of $GeS_{4/2}$ and $Ge_2S_{6/2}$ units in the glass network, and the subsequent formation of bridging S–S linkages in the formation of the latter species. It is the structural reorganization of the matrix associated with the reconfiguration into these units, which

Table 1
Ratios of the different bands at ±1% in the micro-Raman fitted spectrum of the glass $Ge_{0.23}Sb_{0.07}S_{0.70}$ in function of the dose

Dose (MJ/cm^3)	Band at 300 cm^{-1}	Band at 330 cm^{-1}	Band at 340 cm^{-1}	Band at 375 cm^{-1}	Band at 400 cm^{-1}	Band at 425 cm^{-1}
0	13	26	44	6	6	5
18	14	28	40	7	6	5
178	15	38	26	10	6	5
218	15	39	25	10	6	5

can be considered responsible for the photo-expansion seen in Fig. 5. However, Messaddeq et al. have demonstrated that the presence of oxygen is a requirement for creating a volume expansion in glasses in the system Ge–Ga–S [32]. A study of a probable incorporation of Oxygen during the laser irradiation in the investigated glasses is ongoing.

3.3.2. $Ge_{0.23}Sb_{0.07}S_{0.60}Se_{0.10}$ glass

Fig. 10 illustrates the micro-Raman spectra of the glass with $x = 0.10$ before and after irradiation following exposure at different doses. When the dose increases, the intensity of the band at 200 cm^{-1} as well as the bands at 266 and 475 cm^{-1} increase dramatically. The main band (340 cm^{-1}) shifts slightly to lower wavenumbers and becomes broader, while the amplitude of the shoulder at 485 cm^{-1} increases slightly. These two exposure-induced changes are less pronounced than those observed in the pure sulfide glass because of the probable presence of Se in the glass network. Due to its low content compared to S, Se atoms form short Se–Se chains in the germanate sulfide network which may restrict the connection of $GeS_{4/2}$ units by S–S corner sharing. It is possible to think that due to its large size and weaker bond strength, the presence of Se creates a more open network capable of allowing bond distortion upon exposure, rather than major (i.e., bond breaking) conformation changes.

As observed earlier in the purely S-containing glasses, (Fig. 8), the increase of the band at 475 cm^{-1} amplitude has been related to an increase of S–S bonds in rings and can also be seen to undergo changes upon exposure, in the Se-containing materials. The band at 266 cm^{-1} becomes slightly broader when the dose increases suggesting an increase of homopolar Se–Se bonds not only in short chains, but also in rings.

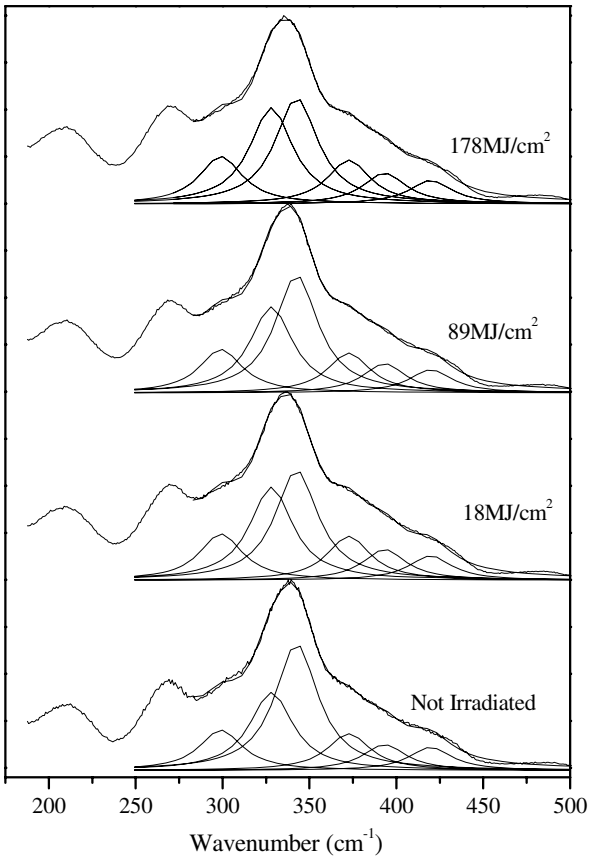

Fig. 11. Deconvolution of the micro-Raman spectra of the glass with $x = 0.10$ after different irradiations.

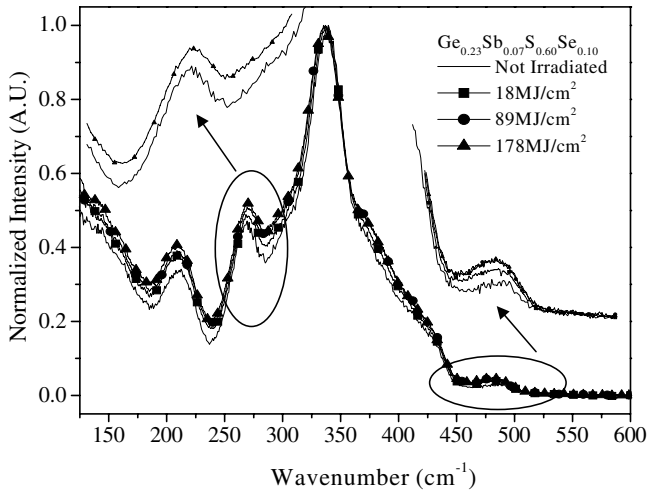

Fig. 10. Micro-Raman spectra of the non-irradiated and irradiated glass with $x = 0.10$.

Fig. 11 presents the fitted micro-Raman spectra for the $x = 0.10$ glass, showing the various contributing bands and their relative fractions. These ratios are summarized in Table 2 and illustrate the subtle change in bonding associated with laser exposure. The intensity of the band at 340 cm^{-1} decreases, while the amplitude of the band at 375 cm^{-1} increases. This suggests that as compared to the sulfide glasses ($x = 0$), the incorporation of selenium in the sulfide network serves to connect edge-sharing $GeS_{4/2}$ units during the laser exposure. The increase of the intensity of the band at 330 cm^{-1} and the decrease of the amplitude of the band at 340 cm^{-1} confirm our interpretation

Table 2
Ratios of the different bands at ±1% in the micro-Raman fitted spectrum of the glass $Ge_{0.23}Sb_{0.07}S_{0.60}Se_{0.10}$ in function of the dose

Dose (MJ/cm^3)	Band at 300 cm^{-1}	Band at 330 cm^{-1}	Band at 340 cm^{-1}	Band at 375 cm^{-1}	Band at 400 cm^{-1}	Band at 425 cm^{-1}
0	13	24	37	11	7	7
18	14	25	32	13	8	7
178	13	28	31	12	9	7
218	14	29	28	13	9	7

that under laser irradiation, a small formation of the corner-sharing $GeS_{4/2}$ units (Fig. 7(a)) increases the number of S–S bridges between GeS_4 tetrahedra. This is verified by the slight increase of the shoulder at 485 cm^{-1} associated with these homopolar bonds. Moreover, the intensity of the band at 375 cm^{-1} does not significantly increase with the progressive increase of the dose as compared to the non-Se containing glass. This shows the poor formation of edge-sharing GeS_4 units (Fig. 7(b)). For this reason, the important increase of the shoulder at 475 cm^{-1} with an increase of the dose may be related, also, to the increase of the band located at around 200 cm^{-1}. Because of the small concentration of Se in the glass network, this band may be related to the vibration of S-rich mixed units like $GeSe_xS_{4-x}$. When the dose increases, some mixed units are expected to connect together or, because of the high concentration of S, link with some GeS_4 units by edge-sharing selenium or sulfur (Fig. 7(b)). Assuming this is the mechanism taking place in this experiment, this may be related to the observed increased formation of homopolar Se–Se and S–S bonds in rings/chains (as seen in the Raman data for post-exposed samples) with an increase of the dose. Because of the low Se content in the glass network, the increase of the band at 266 cm^{-1} with increasing dose suggests that few mixed units $GeSe_{4-x}S_x$ connect by corner sharing Se. Those adjacent regions of Se-containing units which do not participate, is what we expect contribute to the observed increase of homopolar bond Se–Se in chains.

From the evolution of the Raman signal, it appears that the introduction of Se in the germanate network restricts the connection between GeS_4 units through S–S bridges and facilitates the formation of homopolar S–S and Se–Se bonds after laser irradiation. Thus, the increase of the photo-expansion exhibited in Fig. 5 may be correlated to the formation of edge-sharing, S-rich mixed units and also homopolar Se–Se and S–S units. These units are expected to be smaller units compared to the more important number of $GeS_{4/2}$ units connected through a S–S bridge in the Se-free glass explaining the less extensive photo-expansion measured in this glass compared to the Se-free material.

4. Conclusion

The effect of the IR femtosecond laser on the structure of new sulfo-selenide bulk glasses has been studied for the first time. We have shown that these glasses are photo-sensitive to laser irradiation, and exhibit a structural photo-expansion of the sample surface after laser irradiation. We have shown that the photo-sensitivity of the glass as well as the magnitude of photo-expansion depends on glass composition. The increase of the photo-sensitivity of the glass observed with the progressive introduction of Se has been related to the red shift of the absorption band gap. We have demonstrated, through spectroscopic examination, that this photo-response may be related to structural changes with the pure germanate sulfide glass having the largest photo-expansion. Photo-expansion in Se-free and low Se content glasses has been related to the modification of bonding forms under laser irradiation and reorganization of the glass' structural units. Using Raman spectroscopy we have explained that laser irradiation results in an increased connection of GeS_4 units to form corner sharing $GeS_{4/2}$ units within the structure, with a concurrent formation of S–S bridges. The photo-expansion observed in the Se-containing glass may be related to the connection of S-rich mixed units in the glass with a small concentration of Se (10%). The presence and reorganization upon exposure, of the larger fraction of mixed-chalcogen entities results in a larger induced photo-expansion of the glass, compared to the glass with less Se.

This information and the corresponding change in refractive index accompanying this structural modification will allow further evaluation of these new glasses as candidates for waveguide writing.

Acknowledgments

This work has been supported by the National Science Foundation Grants DMR-0321110 and DMR-0312081.

References

[1] K. Hirao, K. Miura, J. Non-Cryst. Solids 239 (1998) 91.
[2] J.W. Chan, T. Huser, S. Risbud, D.M. Krol, Opt. Lett. 26 (2001) 1726.
[3] C.B. Schaffer, A. Brodeur, J.F. Garca, E. Mazur, Opt. Lett. 26 (2001) 93.
[4] A. Zoubir, M. Richardson, C. Rivero, C. Lopez, N. Ho, R. Vallee, K.A. Richardson, in: Conference on Lasers and Electro-Optics (CLEO)OSA Trends in Optics and Photonics Series, vol. 73, Optical Society of America, Washington, DC, 2002, p. 125.
[5] K. Minoshima, A.M. Kowalevicz, I. Hartl, E.P. Ippen, J.G. Fujimoto, Opt. Lett. 26 (2001) 1516.
[6] A. Zoubir, M. Richardson, C. Rivero, C. Lopez, N. Ho, R. Vallee, K.A. Richardson, Technical Digest, Summaries of papers presented at the Conference on Lasers and Electro-Optics, Conference Edition (IEEE Cat. No. 02CH37337) (2002) 125–126.
[7] A. Zoubir, L. Shah, K. Richardson, M. Richardson, Appl. Phys. A 77 (2003) 311.
[8] A. Zoubir, C. Lopez, M. Richardson, K. Richardson, Opt. Lett. 29 (16) (2004) 1840.
[9] A.B. Seddon, J. Non-Cryst. Solids 184 (1995) 44.
[10] C. Meneghini, A. Villeneuve, J. Opt. Soc. Am. B 15 (1998) 2946.
[11] J.M. Harbold, F.O. Ilday, F.W. Wise, J.S. Sanghera, V.Q. Nguyen, L.B. Shaw, I.D. Aggarwal, Opt. Lett. 27 (2002) 119.
[12] Z. Ling, H. Ling, Z. Cheng Shan, J. Non-Cryst. Solids 184 (1995) 1.
[13] H. Nasu, Y. Ibara, .K. Kubodera, J. Non-Cryst. Solids 110 (1989) 229.
[14] J.A. Savage, J. Non-Cryst. Solids 47 (1982) 101.
[15] Znobrik, J. Stetzif, I. Kavich, V. Osipenko, I. Zachko, N. Balota, O. Jakivchuk, Ukr. Phys. J. 26 (1981) 212.
[16] J.-F. Viens, C. Meneghini, A. Villeneuve, T. Galstian, E.J. Knystautas, M.A. Duguay, K.A. Richardson, T. Cardinal, J. Lightwave Technol. 17 (1999) 1184.
[17] G. Fuxi, J. Non-Cryst. Solids 140 (1992) 184.

[18] L. Koudelka, M. Frumar, M. Pisarcik, J. Non-Cryst. Solids 41 (1980) 171.
[19] C. Quemard, F. Smektala, V. Couderc, A. Barthelemy, J. Lucas, J. Phys. Chem. Solids 62 (2001) 1435.
[20] K. Cerqua-Richardson, J.M. McKinley, B. Lawrence, S. Joshi, A. Villeneuve, Opt. Mater. 10 (1998) 155.
[21] T. Cardinal, K.A. Richardson, H. Shim, A. Schulte, R. Beatty, K. Le Foulgoc, C. Meneghini, J.F. Viens, A. Villeneuve, J. Non-Cryst. Solids 256–257 (1999) 353.
[22] L. Petit, N. Carlie, K.C. Richardson, M. Couzi, F. Adamietz, V. Rodriguez, Mater. Chem. Phys. 97 (2006) 64.
[23] C. Lopes, Evaluation of the Photo-induced Structural Mechanism in Chalcogenide Glasses, Ph.D. dissertation, School of Optics, University of Central Florida, Orlando, FL, USA, 2004.
[24] A. Zoubir, Towards Direct Writing of 3D-Photonic Circuits Using Ultrafast Lasers, Ph.D. dissertation, School of Optics, University of Central Florida, Orlando, FL, USA, 2004.
[25] P. Nemec, M. Frumar, J. Jedelsky, M. Jelinek, J. Lancok, I. Gregora, J. Non-Cryst. Solids 299–302 (2002) 1013.
[26] G. Lucovsky, F.L. Galeener, R.C. Keezer, R.H. Geils, H.A. Six, Phys. Rev. B 10 (1974) 5134.
[27] J.E. Griffiths, G.P. Espinosa, J.C. Phillips, J.P. Remeika, Phys. Rev. B 28 (1983) 4444.
[28] Z.G. Ivanova, E. Cernoskova, V.S. Vassilev, S.V. Boycheva, Mater. Lett. 57 (2003) 1025.
[29] B. Frumarova, P. Nemec, M. Frumar, J. Oswald, M. Vleck, J. Non-Cryst. Solids 256&257 (1999) 266.
[30] Q. Mei, J. Saienga, J. Schrooten, B. Meyer, S.W. Martin, J. Non-Cryst. Solids 324 (2003) 264.
[31] C. Julien, S. Barnier, M. Massot, N. Chbani, X. Cai, A.M. Loireau-Lozac'h, M. Guittard, Mater. Sci. Eng. B 22 (1994) 191.
[32] S.H. Messaddeq, V.R. Matestelaro, M. Siu Li, M. Tabackniks, D. Lezal, A. Ramos, Y. Messaddeq, Appl. Surf. Sci. 205 (2003) 143.